Rapid Design Closure of Microwave Components by Means of Feature-Based Optimization and Adjoint Sensitivities

Slawomir Koziel[1,2] and Adrian Bekasiewicz[1,2]

[1] Engineering Optimization & Modeling Center, School of Science and Engineering,
Reykjavik University, Menntavegur 1, 101 Reykjavik, Iceland
(koziel@ru.is, bekasiewicz@ru.is)

[2] Faculty of Electronics, Telecommunications and Informatics,
Gdansk University of Technology, Narutowicza 11/12, 80-233 Gdansk, Poland

Keywords: Microwave design, design closure, EM-driven design, microwave filters, compact circuits, feature-based optimization, adjoint sensitivities.

Abstract

In this paper, fast design closure of microwave components using feature-based optimization (FBO) and adjoint sensitivities is discussed. FBO is one of the most recent optimization techniques that exploits a particular structure of the system response to "flatten" the functional landscape handled during the optimization process, which leads to reducing its computational complexity. When combined with gradient-based search involving adjoint sensitivities, the design cost becomes even lower, allowing us to find the optimum design using just a few electromagnetic (EM) simulations of the structure at hand. Here, operation and performance of the algorithm is demonstrated using a waveguide filter and a miniaturized microstrip rat-race coupler (RRC). Comparative studies indicate considerable savings that can be achieved even compared with adjoint-based gradient search. In case of RRC, numerical results are supported by experimental validation.

1. Introduction

Design closure using full-wave electromagnetic (EM) simulations is nowadays a commonplace and often a necessity in microwave engineering [1], [2]. In many cases, simpler models, such as equivalent circuit ones, provide insufficient accuracy, e.g., due to considerable EM cross-couplings in densely arranged layouts of miniaturized structures [3]. Furthermore, various parasitic phenomena (e.g., skin or proximity effects in case of integrated inductors [4]) or environmental components (connectors [5], or radomes in case of antenna structures [6]) have to be accounted for, which can only be done by means of EM analysis.

Although EM simulation models ensure accuracy (assuming sufficiently dense discretization of the structure at hand), they tend to be computationally expensive even with today's simulation software and hardware. Consequently, EM-driven design closure might be challenging: conventional numerical optimization routines generally require a large number of objective function evaluations, which applies to both gradient-based [7] and derivative-free routines [8], not to mention global algorithms such as population-based metaheuristics [9]-[11]. The high cost issue is more pronounced for complex structures (with longer simulation times) but also for circuits described by a large number of geometry/material parameters that need adjustments.

Various ways of alleviating the difficulties outlined in the previous paragraph have been proposed in the literature. One group of techniques can be categorized as surrogate-based optimization (SBO) [12]. The main concept behind SBO is to shift majority of the operations into a surrogate model which is a computationally cheaper representation of the structure at hand. The expensive EM simulation model is only

referenced to occasionally, primarily for verification purposes as well as to acquire data necessary to enhance the surrogate for subsequent iterations. The surrogates can be constructed as data-driven models (by approximating sampled data from the expensive model [13]) or as physics-based ones (by appropriate correction of the underlying low-fidelity model [3], [14]). The second group is particularly popular in microwave engineering with the most prominent example being space mapping (SM) [14], [15]. In recent years, a number of novel techniques have been developed such as shape-preserving response prediction [16], manifold mapping [12], or adaptive response scaling [17]. The practical issue related to SBO is implementation complexity as well as potential convergence issues [18].

Another approach to lowering the cost of EM-driven design is exploitation of adjoint sensitivities [19]-[21]. Adjoints have been extensively used in other engineering areas since 1980s (e.g., [22], [23]), however, commercial availability of this technology in EM simulation software packages is recent (e.g., [24], [25]). Yet, availability of cheap derivatives already revived interest in gradient-based optimization because it is a simple way of substantial reduction of the optimization cost, as noted in the literature (e.g., [19], [21]). Furthermore, adjoint-based optimization can be further accelerated by combining it with variable-fidelity EM models [26].

One of the recent surrogate-assisted techniques is feature-based optimization (FBO) [27], which exploits the fact that reformulating the design problem in terms of suitably selected characteristic points of the system response allows for considerable computational savings. This is because dependence of these feature point coordinates on

adjustable parameters of the structure at hand is much less nonlinear than that of the original responses such as *S*-parameters versus frequency.

This paper discusses a procedure that allows for combining adjoint-based gradient search with feature-based optimization for further reduction of the computational cost of the design closure. The optimization framework discussed here can be arranged to involve variable-fidelity EM simulation models. Two application examples are considered: a waveguide filter, and a miniaturized rat-race coupler. Significant reduction of the computational cost has been observed of around 40 percent compared to adjoint-based gradient search (without response features). In case of RRC, experimental validation is also provided to confirm reliability of the design process.

2. Variable-Fidelity Design Closure Using Response Features and Adjoint Sensitivities

In this section, we recall formulation of the design problem and discuss the optimization framework involving adjoint sensitivities, variable-fidelity EM models and response features. Demonstration examples have been provided in Section 3.

2.1. Formulation of Design Problem

The design closure task can be formulated as a nonlinear optimization problem of the form

$$\boldsymbol{x}^* = \arg\min_{\boldsymbol{x}} U\left(\boldsymbol{R}_f(\boldsymbol{x})\right) \tag{1}$$

In (1), the symbol $\boldsymbol{R}_f(\boldsymbol{x})$ stands for the response vector of a high-fidelity computational model (here, EM-simulated one) of the structure of interest. In case of filters the responses would normally be return loss and transmission charactersitics versus

frequency; in case of couplers, the response could be, e.g., S_{k1} characteristics as well as a phase shift between the output ports. The vector $\boldsymbol{x}$ represents designable parameters of the problem, typically geometry parameters of the structure. Finally, the scalar function U is a merit function that "measures" the quality of the design (problem dependent).

At a generic level, the optimization algorithm described further may utilize several EM models of various fidelities. The models will be denoted as $\{\boldsymbol{R}_j\}$, $j = 1, \ldots, K$, and are all evaluated using the same EM solver. The model discretization increases for increasing values of j and $\boldsymbol{R}_K = \boldsymbol{R}_f$. Utilization of lower-fidelity model is motivated by potential advantaged from the point of view of computational cost reduction: coarse-discretization simulation is faster so that larger steps in the design space can be made at lower cost. Inaccuracy of the model is corrected by switching to finer discretization at later stages of the process.

In this work, models with different levels of fidelity have been determined based on engineering experience. Given the high-fidelity model, discretization of the lower-fidelity one is reduced while ensuring that it properly captures effects of parametric changes on structure response (e.g., the model reproduces all the resonances that are essential to define feature points). User can decide to construct even more relaxed model assuming that it still represents important features of the structure at hand. Quality of the lower-fidelity model responses w.r.t. high-fidelity one is assessed based on visual inspection. The reason is that norm-wise metrics cannot provide reliable assessment of inaccuracies that can be easily corrected using appropriate techniques (e.g., frequency shifts). It is worth mentioning that preliminary study on automated setup for the low-fidelity models based on correlation analysis has been also performed [33].

2.2. Response Feature Surrogates. Design Problem Re-Formulation

Responses of microwave components (typically, *S*-parameters versus frequency) are highly nonlinear functions of frequency as well as geometry parameters of the structure at hand. This results in slow convergence of the optimization procedures directly controlling such characteristics. As shown in [28], computational speedup can be achieved by reformulating the problem in terms of appropriately defined response features. Figure 1 shows an example of feature point selection for a microwave filter. The points correspond to the edges of the passband (at –20 dB levels) as well as local in-band maxima of the return loss characteristic. Coordinates of these points are sufficient to determine whether the filter satisfies given design specifications, in the example of Fig. 1 defined as $|S_{11}| \leq -20$ dB for 10.4 GHz to 11.6 GHz.

Figure 2 shows a selection of feature points for a microwave coupler. Typically, one is interested in controlling the operating frequency, –20 dB bandwidth, as well as power split. Consequently, the feature points correspond to minimum of matching and isolation characteristics, $|S_{21}|$ and $|S_{31}|$ at the required operating frequency, as well as the frequencies corresponding to –20 dB levels of $|S_{11}|$ and $|S_{41}|$ (necessary for bandwidth calculation).

In more rigorous terms, the feature points of the response vector $\boldsymbol{R}_k(\boldsymbol{x})$ are denoted as $\boldsymbol{p}_k{}^j(\boldsymbol{x}) = [f_k{}^j(\boldsymbol{x})\ r_k{}^j(\boldsymbol{x})]^T$, $j = 1, \ldots, M$. Here, f and r are the frequency and magnitude coordinates of the respective point. A practical way of extracting the characteristic points is simple analysis of the EM-simulated response. For the sake of our numerical experiments, it is realized in Matlab. Feature-based optimization benefits from the fact that dependence of the feature point coordinates on geometry parameters of the structure is less nonlinear

than for the original characteristics. This leads to considerable simplification of the functional landscape to be optimized [28].

According to the FBO paradigm, the problem (1) can be reformulated in terms of the feature points as follows

$$\boldsymbol{x}^* = \arg\min_{\boldsymbol{x}} U_F\left(\boldsymbol{P}_f(\boldsymbol{x})\right) \tag{2}$$

In (2), the function U_F represents design objectives defined in the feature space, which is equivalent to U for the original response $\boldsymbol{R}_f(\boldsymbol{x})$. Furthermore, $\boldsymbol{P}_f = [(\boldsymbol{p}_f^1)^T \ \ldots \ (\boldsymbol{p}_f^M)^T]^T$ represents the vector of aggregated feature points.

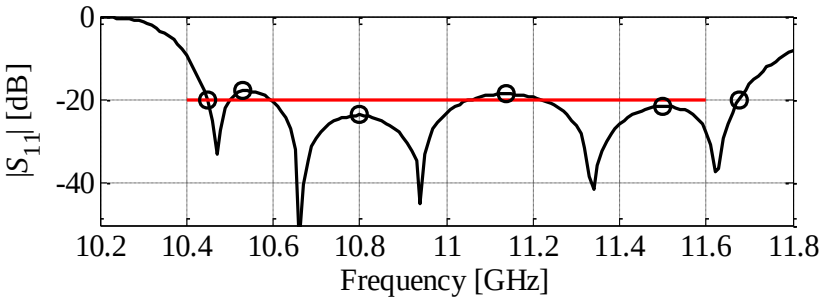

Fig. 1. Response features for microwave filters: filter response (—) and feature points (o), here, corresponding to the edges of the passband (at –20 dB level) as well as local maxima of the in-band ripples. All of these points (and only these) are sufficient to determine violation/satisfaction of design specifications imposed on return loss characteristic. Design specifications marked using a horizontal line.

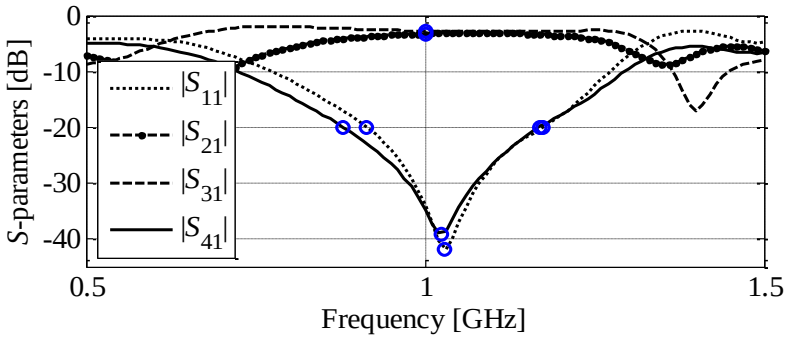

Fig. 2. Response features for coupler structures: minima and –20-dB-levels points of $|S_{11}|$ and $|S_{41}|$ as well as $|S_{21}|$ and $|S_{31}|$ values at the required operating frequency. These points are sufficient to determine satisfaction/violation of the design specs concerning the operating frequency, bandwidth, as well as power split.

2.3. Optimization Algorithm

The variable-fidelity feature-based optimization algorithm involving adjoint sensitivities is an iterative procedure that generates a sequence of approximate solutions to (1), $\boldsymbol{x}^{(j)}$, $j = 0, 1, \ldots, K$, as follows

$$\boldsymbol{x}^{(1)} = \arg\min_{\boldsymbol{x}} U(\boldsymbol{R}_1(\boldsymbol{x})) \tag{3}$$

and

$$\boldsymbol{x}^{(j)} = \arg\min_{\boldsymbol{x}} U_F(\boldsymbol{P}_j(\boldsymbol{x})) \tag{4}$$

for $j > 1$. More specifically, the design $\boldsymbol{x}^{(j)}$ is an optimum of the jth model $\boldsymbol{R}_j$. The final outcome of the optimization process is $\boldsymbol{x}^{(K)} = \boldsymbol{x}^*$. The sub-problem (3) is solved at the level of the original responses, which is due to the fact that when away from the optimum, the response structure can be different from that close to the final design and the feature points may not be well defined.

Both sub-problems (3) and (4) are solved in an iterative manner as follows

$$\boldsymbol{x}^{(1,i+1)} = \arg\min_{\boldsymbol{x}:\|\boldsymbol{x}-\boldsymbol{x}^{(1,i)}\|\le\delta^{(1,i)}} U(\boldsymbol{G}_1^{(i)}(\boldsymbol{x})) \tag{5}$$

and

$$\boldsymbol{x}^{(j,i+1)} = \arg\min_{\boldsymbol{x}:\|\boldsymbol{x}-\boldsymbol{x}^{(j,i)}\|\le\delta^{(j,i)}} U_F(\boldsymbol{H}_j^{(i)}(\boldsymbol{x})) \tag{6}$$

In the above equations, the vector $\boldsymbol{x}^{(j,i)}$, $i = 0, 1, \ldots$, represent approximations to the solution of (3) (for $j = 1$) and (4) (for $j > 1$). The model $\boldsymbol{G}_1^{(i)}$ is the linear expansion of the EM-model $\boldsymbol{R}_1$ at $\boldsymbol{x}^{(1,i)}$ defined as

$$\boldsymbol{G}_j^{(i)}(\boldsymbol{x}) = \boldsymbol{R}_j(\boldsymbol{x}^{(i)}) + \boldsymbol{J}_{\boldsymbol{R}_j}(\boldsymbol{x}^{(j,i)}) \cdot (\boldsymbol{x} - \boldsymbol{x}^{(j,i)}) \tag{7}$$

Similarly, the model $\boldsymbol{H}_j^{(i)}$ is the first-order expansion of the feature vector $\boldsymbol{P}_j$:

$$\boldsymbol{H}_j^{(i)}(\boldsymbol{x}) = \boldsymbol{P}_j(\boldsymbol{x}^{(i)}) + \nabla_{\boldsymbol{P}_j}(\boldsymbol{x}^{(j.i)}) \cdot (\boldsymbol{x} - \boldsymbol{x}^{(j.i)}) \tag{8}$$

The derivatives of the respective models (Jacobian $\boldsymbol{J}_{\boldsymbol{R}1}$ of $\boldsymbol{R}_1$ and feature point gradients $\nabla_{\boldsymbol{P}j}$ of $\boldsymbol{P}_j$) are obtained using adjoint sensitivities.

The results of the previous iteration are used as a starting point for the next optimization stage, i.e., we have $\boldsymbol{x}^{(j.0)} = \boldsymbol{x}^{(j-1)}$. The user-supplied initial design $\boldsymbol{x}^{(0)}$ is the starting point for optimizing the first model $\boldsymbol{R}_1$.

The optimization algorithm is embedded in the trust-region (TR) framework [29], where optimization of the linear expansion models is restricted to the vicinity of the current design of the size $\delta^{(j.i)}$. Updating of the TR radius follows the standard rules and it is based on the gain ratio calculated as the ratio of the actual versus predicted improvement of the objective function value [29].

An important factor is the strategy for switching between the models. This is controlled by the termination condition $\| \boldsymbol{x}^{(j.i)} - \boldsymbol{x}^{(j.i-1)} \| < \varepsilon_j$, where $\varepsilon_j = M^{(K-j)}\varepsilon$, with ε being the overall termination threshold, here, $\varepsilon = 0.001$, and M being the scaling factor (here, we use $M = 10$). In other words, the termination condition for optimizing lower-fidelity models is more relaxed than for the higher-fidelity ones. The motivation is that due to the limited accuracy of coarse-discretization simulations, there is no need aim at precise allocation of the optimum design for such models.

Although the generic methodology described above utilized auxiliary coarse-discretization EM models, in principle, it is possible to only utilize one model (the high-fidelity one), i.e., $K = 1$. Illustration of this is provided in Section 3 using the second verification example.

3. Case Studies

In this section, the design optimization framework has been demonstrated using two cases, a coupler iris waveguide filter and a miniaturized rat-race coupler. For first example, variable-fidelity models are utilized, whereas the last test case only exploits the high-fidelity model.

3.1. Four-Aperture Iris Coupled Bandpass Filter

Our first design case is a four-aperture iris coupled bandpass filter shown in Fig. 3 [30]. The structure is implemented in WR-90 waveguide. The vector of design parameters is $\boldsymbol{x} = [z_1\ x_1\ x_2\ s_{x1}\ s_{x2}\ s_{y1}\ s_{y2}\ z_{t1}\ z_{t2}]^T$ (all in mm). The EM model of the filter is prepared and evaluated in HFSS [25]. Optimization of the considered filter is performed using variable-fidelity EM model framework (K = 3; cf. Section 2). Feature points for the structure have been located at the edges of the passband (at –20 dB levels) as well as local in-band maximum of the reflection response (cf. Fig. 4).

We utilize two coarsely-discretized EM surrogates, i.e., $\boldsymbol{R}_1$ that contains about 6,000 tetrahedral cells and $\boldsymbol{R}_2$ with ~19,000 cells. Their average simulation times on a dual Xeon E5540 machine with 64 GB of RAM are about 3 min and 10 min, respectively. We also use the high-fidelity model $\boldsymbol{R}_f$ consisting of ~150,000 cells (simulation time 40 minutes). The design objective is to minimize the structure reflection below –20 dB in 14.9 GHz to 15.1 GHz range.

The initial design is $\boldsymbol{x}^{(0)} = [12.5\ 5.0\ 5.0\ 2.5\ 2.5\ 0.5\ 0.0\ 0.25\ 0.25]^T$ mm. The filter has been optimized using method of Section 2. The final dimensions of the structure $\boldsymbol{x}^* = [11.63\ 5.03\ 5.07\ 2.41\ 2.149\ 0.497\ –0.068\ 0.201\ 0.206]^T$ mm have been obtained a

cost corresponding to just six evaluations of the high-fidelity model (cf. Table 1). Comparison of the $\boldsymbol{R}_f$ model responses at the initial and optimized designs is shown in Fig. 4. It should be noted that, despite poor quality of the $\boldsymbol{x}^{(0)}$, "flattening" of the functional landscape by FBO allows for obtaining the final design at a low cost.

For the sake of comparison, the considered filter has been also optimized using trust-region frameworks with (i) variable-fidelity models, and (ii) only the high-fidelity model (ii). Both benchmark approaches exploit sensitivity data. A summary of the optimization results for considered methods is given in Table 1. It should be noted that benchmark techniques yield comparable designs but at higher cost (by 47% and 233% for (i) and (ii), respectively).

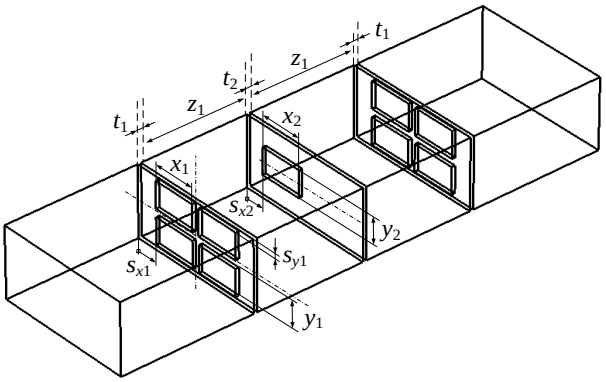

Fig. 3. Geometry of the four-aperture iris coupled bandpass filter [30].

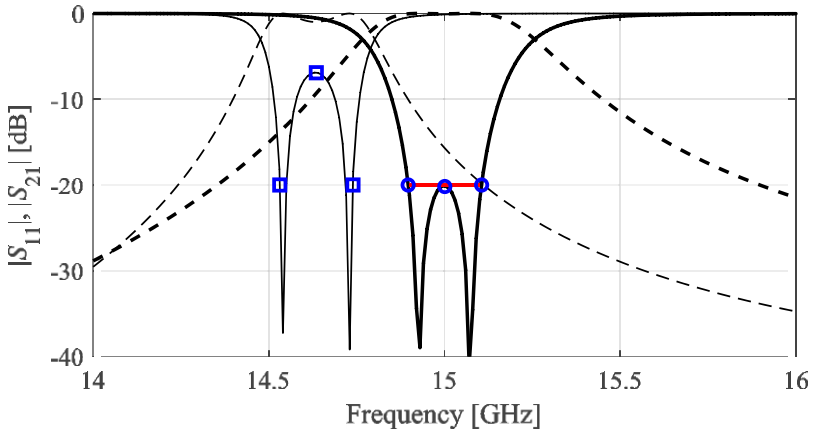

Fig. 4. High-fidelity model responses of the four-aperture iris coupled bandpass filter at the initial (thin lines) and optimized (thick lines) designs: $|S_{11}|$ (—) and $|S_{21}|$ (– –). Squares and circles represent feature points at the initial and final design, respectively.

Table 1. Four-Aperture Iris Coupled Bandpass Filter: Optimization Results

Design Method	Design Cost			max $\|S_{11}\|$ for 10.4 GHz to 11.6 GHz at Optimized Design
	Number of Evaluations	Absolute [min]	Relative to $\boldsymbol{R}_f$	
Variable-Fidelity FBO (This work)	$11 \times \boldsymbol{R}_1$	33	0.8	–20.4 dB
	$5 \times \boldsymbol{R}_2$	50	1.2	
	$4 \times \boldsymbol{R}_f$	160	4.0	
	Total cost:	243	6.0	
Variable-Fidelity Trust-Region[$]	$11 \times \boldsymbol{R}_1$	33	0.8	–23.5 dB
	$8 \times \boldsymbol{R}_2$	80	2.0	
	$6 \times \boldsymbol{R}_f$	240	6.0	
	Total cost:	353	8.8	
Trust-Region-Based[#]	$20 \times \boldsymbol{R}_f$	800	20.0	–23.0 dB

[$] Optimization with adjoint sensitivities (with $K = 3$).
[#] Optimization of $\boldsymbol{R}_f$ with adjoints (cf. Section 2 with $K = 1$).

3.2. Compact Microstrip Rat-Race Coupler

Our second example is a miniaturized microstrip 3 dB rat-race coupler (RRC) shown in Fig. 5 [31]. The circuit is composed of two different compact microstrip resonant cells. RRC is designed on a 0.762 mm thick Taconic RF-35 dielectric substrate (ε_r = 3.5, tanδ = 0.0018). The vector of design parameters is $\boldsymbol{x} = [w_1\ w_2\ w_3\ d_1\ d_2\ l_1]^T$. Dimension w_0 = 1.7 remains fixed to ensure 50 ohm input impedance. The EM model of the structure is implemented in CST Microwave Studio and simulated using its transient solver. The model contains about 330,000 tetrahedral mesh cells and its average simulation time is 6 min.

The following design requirements are assumed with respect to matching (S_{11}), transmission (S_{21}), coupling (S_{31}), and isolation (S_{41}):

- maximization of bandwidth (BW) defined as a symmetric—with respect to the center frequency of 1 GHz—part of the response for which both $|S_{11}|$ and $|S_{41}|$ are below –20 dB;

- reducing the power split error at the center frequency $d_S = |S_{21.f}(\boldsymbol{x}) - S_{31.f}(\boldsymbol{x})|$ to zero;
- maintaining possibly small shift of the resonances $S_{11.f}(\boldsymbol{x})$ and $S_{41.f}(\boldsymbol{x})$ with respect to the operating frequency.

It should be noted that maximization of bandwidth is a primary objective, whereas the remaining requirements are handled as constraints. Here, they are incorporated into the objective using penalty functions [11].

The considered structure has been optimized using the technique of Section 2 assuming $K = 1$ (i.e., no auxiliary lower-fidelity models). The initial design is $\boldsymbol{x}^0$ = [4.0 0.3 2.0 0.3 0.2 1.0]^T. The optimized coupler design is $\boldsymbol{x}^*$ = [3.87 0.43 1.76 0.37 0.36 1.10]^T. It should be noted that, due to "flattening" of the functional landscape, final RRC design has been obtained in just six iterations of the feature-based algorithm at a cost of only 8 EM model evaluations. A comparison of the structure responses at the initial and final designs is shown in Fig. 6. The results indicate that, for the optimized design, the –20 dB bandwidth of 343 MHz has been obtained together with power split error of 0.15 dB and acceptable resonances shifts. The size of the optimized structure is 470 mm^2 which is over 90% smaller compared to conventional rectangular RRC [32].

The coupler has been also optimized at the level of frequency responses using adjoints-based gradient search embedded in trust-region framework (also with $K = 1$, cf. Section 2). Although the obtained design is similar (BW: 341 MHz, 3 dB error: 0.15 dB, and footprint: 472 mm^2), it has been obtained at a cost of 13 evaluations of the structure EM model (eight algorithm iterations). In other words, combining adjoints with FBO results in almost 40% computational cost savings.

Figure 7 shows the results of experimental validation of the optimized RRC. It can be observed that the agreement between simulation and measurements is good. Visible discrepancies between responses are mostly due to utilization of simplified EM model that lacks SMA connectors, as well as fabrication tolerances.

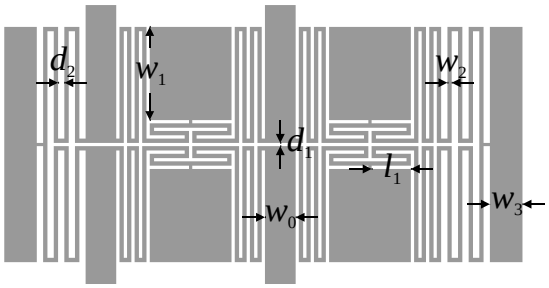

Fig. 5. A compact RRC composed of compact microstrip resonant cells [31].

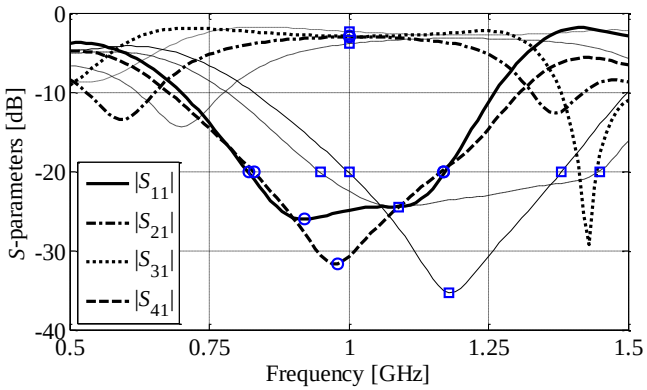

Fig. 6. Compact rat-race coupler: frequency responses at the initial (thin lines) and final designs (thick lines). Squares and circles represent feature points at the initial and final designs, respectively.

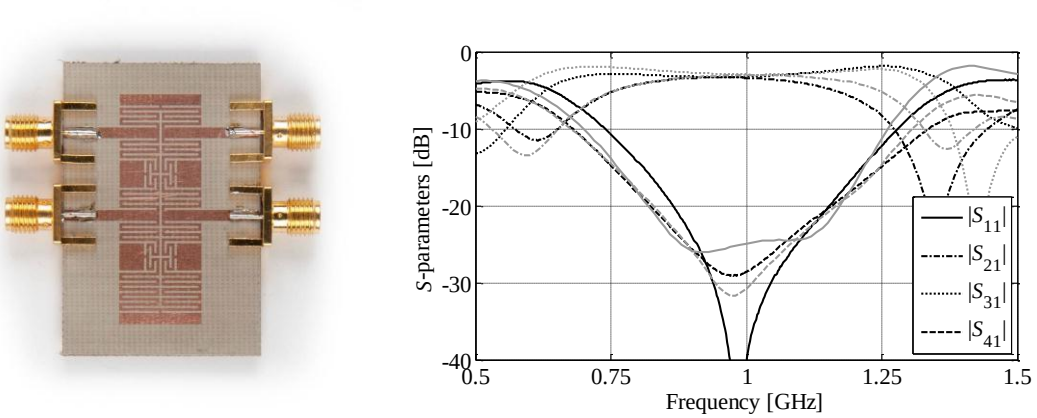

Fig. 7. Experimental validation of the RRC: (a) photograph of the fabricated coupler prototype, (b) simulated (gray) and measured (black) coupler characteristics.

4. Conclusion

Application of feature-based optimization, variable-fidelity EM simulations and adjoint sensitivities for rapid design closure of microwave components have been discussed. Numerical results indicate that the aforementioned computation allows for significant reduction of the computational cost of the optimization process, even compared with gradient-based search with adjoints by about 40 percent. The future work with be focused on application of the framework for other demanding problems, including design closure of antennas and antenna arrays.

Acknowledgement

The authors thank Computer Simulation Technology AG, Darmstad Germany for making CST Microwave Studio available. This work is partially supported by the Icelandic Centre for Research (RANNIS) Grant 174114051, and by National Science Centre of Poland Grant 2015/17/B/ST6/01857.

References

[1] Y. Wang, K. Ma, N. Yan, and L. Li, "A slow-wave rat-race coupler using substrate integrated suspended line technology," *IEEE Trans. Components, Packaging and Manufacturing Technol.*, vol. 7, no. 4, pp. 630-636, 2017.

[2] C.C. Chen, C.Y.D. Sim, and Y.J. Wu, "Miniaturised dual-band rat-race coupler with harmonic suppression using synthetic transmission line," *Electronics Lett.*, vol. 52, no. 21, pp. 1784-1786, 2016.

[3] S. Koziel, A. Bekasiewicz, and P. Kurgan, "Rapid design and size reduction of microwave couplers using variable-fidelity EM-driven optimization," *Int. J. RF Microwave CAE*, vol. 26, no. 1, pp. 27-35, 2016.

[4] X. Xu, P. Li, M. Cai, and B. Han, "Design of novel high-Q-factor multipath stacked on-chip spiral inductors," *IEEE Trans. Electron Devices*, vol. 59, no. 8, pp. 2011-2018, 2012.

[5] A. Bekasiewicz and S. Koziel, "Cost-efficient design optimization of compact patch antennas with improved bandwidth," *IEEE Ant. Wireless Prop. Lett.*, vol. 15, pp. 270-273, 2016.

[6] B. Wang, M. He, J. Liu, H. Chen, G. Zhao, and C. Zhang, "An efficient integral equation/modified surface integration method for analysis of antenna-radome structures in receiving mode," *IEEE Trans. Ant. Prop.*, vol. 62, no. 9, pp. 4884-4889, 2014.

[7] J. Nocedal and S. Wright, *Numerical Optimization*, 2nd edition, Springer, New York, 2006.

[8] A. Conn, K. Scheinberg, and L.N. Vincente, *Introduction to Derivative-Free Optimization*, MPS-SIAM Series on Optimization, Philadelphia, 2009.

[9] S. Chamaani, M.S. Abrishamian, and S.A. Mirtaheri, "Time-domain design of UWB Vivaldi antenna array using multiobjective particle swarm optimization," *IEEE Ant. Wireless Prop. Lett.*, vol. 9, pp. 666-669, 2010.

[10] Q. Wang and S.T. Ho, "Ultracompact multimode interference coupler designed by parallel particle swarm optimization with parallel finite-difference time-domain," *J. Lightwave Technol.*, vol. 28, no. 9, pp. 1298-1304, 2010.

[11] H. Ghorbaninejad and R. Heydarian, "New design of waveguide directional coupler using genetic algorithm," *IEEE Microwave Wireless Comp. Lett.*, vol. 26, no. 2, pp. 86-88, 2016.

[12] S. Koziel, D. Echeverría-Ciaurri, and L. Leifsson, "Surrogate-based methods," in S. Koziel and X.S. Yang (Eds.) *Computational Optimization, Methods and Algorithms*, Series: Studies in Computational Intelligence, Springer-Verlag, pp. 33-60, 2011.

[13] N.V. Queipo, R.T. Haftka, W. Shyy, T. Goel, R. Vaidynathan, and P.K. Tucker, "Surrogate-based analysis and optimization," *Prog. Aerospace Sci.*, vol. 41, no. 1, pp. 1-28, Jan. 2005.

[14] J.W. Bandler, Q.S. Cheng, N.K. Nikolova, and M.A. Ismail, "Implicit space mapping optimization exploiting preassigned parameters," *IEEE Trans. Microwave Theory Tech.*, vol. 52, no. 1, pp. 378-385, 2004.

[15] J.W. Bandler, Q.S. Cheng, S.A. Dakroury, A.S. Mohamed, M.H. Bakr, K. Madsen, and J. Søndergaard, "Space mapping: the state of the art," *IEEE Trans. Microwave Theory Tech.*, vol. 52, no. 1, pp. 337-361, 2004.

[16] S. Koziel, S. Ogurtsov, and S. Szczepanski, "Rapid antenna design optimization using shape-preserving response prediction," *Bulletin of the Polish Academy of Sciences. Tech. Sci.*, vol. 60, pp. 143-149, 2012.

[17] S. Koziel and A. Bekasiewicz, "Rapid microwave design optimization using adaptive response scaling," *IEEE Trans. Microwave Theory Tech.*, vol. 64, no. 9, pp. 2749-2757, 2016.

[18] S. Koziel, J.W. Bandler, and K. Madsen, "Quality assessment of coarse models and surrogates for space mapping optimization," *Opt. Eng.*, vol. 9, no. 4, pp. 375-391, 2008.

[19] S. Koziel, F. Mosler, S. Reitzinger, and P. Thoma, "Robust microwave design optimization using adjoint sensitivity and trust regions," *Int. J. RF and Microwave CAE*, vol. 22, no. 1, pp. 10-19, 2012.

[20] M.H. Bakr and N.K. Nikolova, "An adjoint variable method for time domain TLM with wideband Johns matrix boundaries," *IEEE Trans. Microwave Theory Tech.*, vol. 52, no. 2, pp. 678-685, 2004.

[21] A. Bekasiewicz and S. Koziel, "Efficient multi-fidelity design optimization of microwave filters using adjoint sensitivity," *Int. J. RF and Microwave CAE*, 25, no. 2, pp. 178-183, 2015.

[22] A. Jameson, "Aerodynamic design via control theory," *Journal of Scientific Computing*, vol. 3, pp. 233-260, 1988.

[23] C. Mader, J. Martins, J.J. Alonso, and E. van der Weide, "ADjoint: an approach for the rapid development of discrete adjoint solvers," *AIAA Journal*, vol. 46, no. 4, pp. 863-873, April 2008.

[24] CST Microwave Studio, ver. 2013, CST AG, Bad Nauheimer Str. 19, D-64289 Darmstadt, Germany, 2013.

[25] Ansys HFSS, ver. 14.0, ANSYS, Inc., Southpointe 275 Technology Drive, Canonsburg, PA 15317, 2012.

[26] S. Koziel and A. Bekasiewicz, "Rapid design optimization of antennas using variable-fidelity EM models and adjoint sensitivities," *Engineering Computations*, vol. 33, no. 7, pp. 2007-2018, 2016.

[27] S. Koziel and S. Ogurtsov, "Fast surrogate-assisted simulation-driven optimisation of add-drop resonators for integrated photonic circuits," *IET Microwaves, Ant. Prop.*, vol. 9, no. 7, pp. 672-675, 2015.

[28] A. Bekasiewicz and S. Koziel, "Response features and circuit decomposition for accelerated EM-driven design of compact impedance matching transformers," *Microwave Opt. Tech. Lett.*, vol. 58, no. 9, pp. 2130-2133, 2016.

[29] A. Conn, N.I.M. Gould, and P.L. Toint, *Trust-region methods*, MPS-SIAM Series on Optimization, Philadelphia, 2000.

[30] W. Hauth, R. Keller, U. Papziner, R. Ihmels, T. Sieverding, and F. Arndt, "Rigorous CAD of multipost coupled rectangular waveguide components," *Proc. European Microw. Conf.*, pp. 611-614, Madrid, 1993.

[31] S. Koziel and A. Bekasiewicz, "Novel structure and size-reduction-oriented design of microstrip compact rat-race coupler," *Int. Rev. Prog. Applied Comp. EM*, pp. 1-2, Honolulu, 2016.

[32] A. Bekasiewicz, S. Koziel, and B. Pankiewicz, "Accelerated simulation-driven design optimisation of compact couplers by means of two-level space mapping," *IET Microwaves, Ant. Prop.*, vol. 9, no. 7, pp. 618-626, 2015.

[33] S. Koziel and A. Bekasiewicz, "Variable-fidelity design optimization of antennas with automated model selection," *European Conference on Antennas and Propagation*, pp. 1-5, Davos, 2016.